

The Impact of Diabetes Mellitus on the Osseointegration of Absorbable Screws: An Animal Experimental Investigation

(Kesan Diabetes Melitus terhadap Osseointegrasi Skru Boleh Serap: Suatu Penyelidikan Uji Kaji Haiwan)

ZELIN WU¹, LEI XIAO¹, HUIGE HOU¹, LING LI², YANPING GAO³, JIAN GUAN⁴, JIWEN CHEN⁵, LINGFENG ZENG⁶, ZIHANG CHEN⁷, TSZ-NGAI MOK⁸, GUIQIANG MIAO⁹, XIAOFEI ZHENG^{1,*}, SHIGUO YUAN¹⁰ & HUAJUN WANG¹

¹*Department of Sports Medicine, The First Affiliated Hospital, Guangdong Provincial Key Laboratory of Speed Capability, The Guangzhou Key Laboratory of Precision Orthopedics and Regenerative Medicine, Jinan University, Guangzhou 510630, China*

²*Department of Rheumatology and Immunology, Guangdong Provincial People's Hospital (Guangdong Academy of Medical Sciences), Southern Medical University, Guangzhou 510080, China*

³*Department of Traditional Chinese Orthopedics and Traumatology, Center for Orthopaedic Surgery, The Third Affiliated Hospital of Southern Medical University, Guangzhou 510630, China*

⁴*Department of Orthopedics, The Third Hospital of Shijiazhuang, Shijiazhuang 050011, China*

⁵*Department of Orthopedics, The Affiliated Shunde Hospital of Jinan University, Foshan 528000, China*

⁶*The Second Affiliated Hospital of Guangzhou University of Chinese Medicine (Guangdong Provincial Hospital of Chinese Medicine), Guangzhou 510120, China*

⁷*Department of Psychology, Li Ka Shing Faculty of Medicine, State Key Laboratory of Brain and Cognitive Sciences, The University of Hong Kong, Hong Kong SAR 999077, China*

⁸*The City University of Hong Kong, Hong Kong SAR 999077, China*

⁹*Department of Orthopedics, Foshan Fosun Chancheng Hospital, Foshan 528031, China*

¹⁰*Department of Orthopaedic, Hainan Hospital, Guangdong Provincial Hospital of Chinese Medicine, Guangzhou University of Chinese Medicine, Affiliated Hospital of Chinese Medicine, Hainan Medical University, Haikou 570100, China*

Received: 23 September 2024/Accepted: 26 November 2024

ABSTRACT

This study aims to explore the correlation between alterations in blood glucose levels and the osseointegration as well as biomechanical properties of nHA/PLLA absorbable screws, and elucidate the impact of DM on bone metabolism surrounding nHA/PLLA absorbable screws. 75 rats were randomly assigned to either the Diabetes mellitus (DM) group and the control group. DM was induced in rats through intraperitoneal injection of 1% streptozotocin. A single nHA/PLLA absorbable screw was surgically implanted into the medial tibia of each rat in both groups. Rats were euthanized at 4 weeks, 8 weeks and 12 weeks post-implantation, and tissue specimens were subjected to histological, histomorphological, Micro-CT scan, biomechanical, microindentation mechanical testing of trabeculae bone, Raman spectroscopy, and Western blot analyses. Changes in bone mass, trabeculae structure, composition, mechanical properties, and expression of bone formation-related proteins around the absorbable screws were compared between the two groups at the microscopic, biomechanical, and molecular levels. The results show that DM disrupts the trabeculae structure surrounding absorbable screws, leading to alterations in trabeculae bone composition, diminished mechanical properties, and impaired bone metabolism. DM significantly compromises osseointegration at the absorbable screw-bone interface and diminishes bone quality in the vicinity of the absorbable screw.

Keywords: Absorbable screw; diabetes mellitus; nHA/PLLA; osseointegration

ABSTRAK

Penyelidikan ini bertujuan untuk meneroka korelasi antara perubahan paras glukosa darah dan osseointegrasi serta sifat biomekanikal skru boleh diserap nHA/PLLA dan menjelaskan kesan DM pada metabolisme tulang di sekeliling skru boleh diserap nHA/PLLA. Tujuh puluh lima tikus secara rawak ditandatangani sama ada kepada kumpulan Diabetes melitus (DM) dan kumpulan kawalan. DM telah diinduksi pada tikus melalui suntikan intraperitoneal 1% streptozotocin. Satu skru boleh diserap nHA/PLLA telah ditanam secara pembedahan ke dalam tibia medial setiap tikus dalam kedua-dua kumpulan. Tikus telah dikorbankan pada 4 minggu, 8 minggu dan 12 minggu selepas implantasi dan spesimen tisu tertakluk kepada histopologi, histomorfologi, imbasan Mikro-CT, biomekanikal, ujian mekanikal lekukan mikro tulang trabekula,

spektroskopi Raman dan analisis pembloatan Western. Perubahan dalam jisim tulang, struktur trabekula, komposisi, sifat mekanikal dan ekspresi protein berkaitan pembentukan tulang di sekeliling skru yang boleh diserap dibandingkan antara kedua-dua kumpulan pada tahap mikroskopik, biomekanikal dan molekul. Keputusan menunjukkan bahawa DM mengganggu struktur trabekula di sekeliling skru yang boleh diserap yang membawa kepada perubahan dalam komposisi tulang trabekula, sifat mekanikal yang berkurangan dan metabolisme tulang terjejas. DM secara ketara menjejaskan proses osseointegrasi pada antara muka skru boleh serap-tulang dan merendahkan kualiti tulang di sekitar skru tersebut.

Kata kunci: Diabetes melitus; nHA/PLLA; osseointegrasi; skru yang boleh diserap

INTRODUCTION

With the advancements in materials science, nano-hydroxyapatite/poly-L-lactic acid (nHA/PLLA) absorbable screws have gained increasing utilization in orthopedics and sports medicine. The biodegradable nature of these screws alleviates the need for secondary nail removal, reduces foreign body reactions, and enhances compatibility with surrounding bone tissue. Notably, they find applications in treating conditions such as rotator cuff injuries, anterior and posterior cruciate ligament tears of the knee joint, long bone fractures, and spinal fractures (Arama et al. 2015; Kim et al. 2015; Macarini et al. 2008). However, their susceptibility to the physiological environment may pose a challenge, as abnormal degradation rates resulting from inflammatory metabolic conditions are a significant factor contributing to surgical failures (Galiveeti, El-Abed & Ahmad 2023; Palumbo, Kuzma & Flanigan 2023).

Diabetes mellitus (DM), a disease characterized by ineffective insulin production or utilization leading to elevated blood glucose levels, is a growing health concern globally. Urbanization, aging demographic, reduced physical activity, and increasing rates of overweight and obesity contribute to the escalating prevalence of DM (International Diabetes Federation 2024). According to the International Diabetes Federation (IDF) (2024), approximately 10.5% of the world's adult population (ages 20 - 79) had DM in 2021, with nearly half of them undiagnosed. In addition, the IDF made a projection in 2024 that approximately one in eight adults (approximately 783 million) will be affected by diabetes by 2045, posing a major challenge for individuals, families and countries globally.

Osseointegration, defined as the direct contact between an implant and surrounding bone tissue without interposed fibrous tissue, which is a structural and functional connection, represents a critical aspect of successful internal fixation. Optimal osseointegration facilitates the integration of artificial implants with surrounding tissue, enhancing internal fixation stability and reducing failure rates. Research indicates that DM adversely affects osseointegration, characterized by disrupted bone tissue architecture, diminished new bone formation, reduced maturity and continuity, altered bone trabeculae parameters, and decreased expression of growth factors. For examination, clinical evidence from orthopedic and dental departments highlights an increased risk of titanium alloy screw failure in DM patients compared

to non-DM individuals (Corrêa et al. 2021; Xiang et al. 2020). Moreover, DM patients are at a significantly higher risk of screw loosening, predominantly occurring within the first year post-implantation (Mellado-Valero et al. 2007). Animal study demonstrate that elevated blood glucose levels significantly impede new bone formation around titanium alloy screws (Shyng, Devlin & Ou 2006). And effective glycemic control in DM rats improves osseointegration between titanium alloy screws and bone (Kwon et al. 2005). Previous research conducted by our group further corroborates the detrimental effect of DM on osseointegration with titanium screws, evidenced by disorganized and sparse bone tissue arrangement, reduced new bone formation, and compromised maturity and continuity (Xiao 2019). Nonetheless, existing studies predominantly focus on the impact of DM on conventional metal screws, with a notable dearth of experimental and clinical investigations regarding its effect on osseointegration of nHA/PLLA absorbable screws.

This study aimed to explore the interplay between DM and the biomechanical robustness of osseointegration with nHA/PLLA absorbable screws. Additionally, it sought to elucidate the impact of DM on bone metabolism surrounding nHA/PLLA absorbable screws and to furnish experimental evidence addressing clinical queries, including the advisability of recommending nHA/PLLA absorbable screws and the potential benefits of hypoglycemic medications in enhancing osseous integration among DM patients.

MATERIALS AND METHODS

EXPERIMENTAL ANIMAL GROUPING AND EXPERIMENTAL DESIGN

A cohort of 75 healthy male Sprague-Dawley (SD) rats, aged 2 months and weighing between 220 g and 260 g, was procured from the Medical Animal Laboratory Center of Jinan University. These rats were exclusively sourced from and housed at the aforementioned facility, where all experimental procedures were conducted in accordance with protocols approved by the Animal Experiment Ethics Committee of Jinan University (20180531-07). Subsequently, the rats were randomly assigned to either the DM group (n = 45) or the control group (n = 30). Following this, each group was further subdivided into 4 weeks (4W), 8 weeks (8W) and 12 weeks (12W) cohorts.

Upon animal arrival, the rats underwent one week acclimatization period at the animal experimental center to allow them to become familiar with their new surroundings. In the DM group, type 1 DM was induced via intraperitoneal administration of 1% streptozotocin (STZ), with weekly blood glucose measurements used to confirm DM status. Meanwhile, rats of control group received intraperitoneal injections of citrate buffer. Following two weeks interval, surgical implantation of nHA/PLLA absorbable screws was performed in the medial tibia of both groups. Thereafter, rats were euthanized at 4 weeks, 8 weeks, and 12 weeks post-implantation, and tissue specimens were collected for subsequent analysis.

ESTABLISHMENT OF RAT MODEL OF TYPE 1 DM

Prior to commencing the modeling procedure, rats underwent assessment of random blood glucose levels to ensure baseline normoglycemia. Following an overnight fast lasting 8 - 12 h, rats assigned to the DM group received intraperitoneal injections of 1% STZ at a dosage of 120 mg/kg, dissolved in a solution comprising 0.1 mol/L citrate solution (54 mL) and 0.1 mol/L sodium citrate solution (46 mL) adjusted to a pH of 4.4. Control rats received equivalent injections of citrate buffer. During injection, careful attention was paid to positioning the rat's head downward and elevating the abdomen, with the injection site selected in the posterior one-third of the lower abdomen to minimize the risk of bladder puncture. Following injection, iodophor and erythromycin ointment were applied to the injection site to mitigate the risk of localized infection. Monitoring for hypoglycemic convulsions was conducted 6 - 10 h post-STZ administration, with immediate intervention provided as needed to prevent adverse outcomes. Given the propensity for STZ aqueous solution to undergo decomposition, fresh solutions were prepared onsite to minimize exposure time and maintain solution integrity. Blood glucose levels were assessed at 2 days, 3 days, 7 days and 14 days post-STZ injection. The DM model was deemed established when random blood glucose levels exceeded 16.7 mmol/l in the DM group, accompanied by characteristic symptoms such as polyuria, polydipsia, increased food intake, and weight loss. Rats failing to meet these criteria were excluded from the study. Successful DM rats were provided with adequate food and water, and daily bedding changes were conducted to uphold cage hygiene and prevent potential disease or infection, given the increased urine production observed in DM rats.

ESTABLISHMENT OF SCREW IMPLANTATION ANIMAL MODEL

Male SD rats allocated to both the DM and control groups, underwent weighing and subsequent anesthesia induction via intramuscular injection of 1.5% pentobarbital sodium at a dosage of 2 mL/kg, adjusted according to individual body weights. Following anesthesia induction, the rats

were meticulously positioned in the supine orientation on the operating table. Preoperative preparation encompassed thorough skin cleansing overlying both knee joints, followed by meticulous disinfection of the surgical sites utilizing 0.5% iodophor disinfectant, with subsequent application of conventional gauze for coverage. Surgical intervention commenced with a longitudinal incision of approximately 1 cm over the upper tibia, accompanied by systematic layer-by-layer dissection of the overlying skin and subcutaneous tissue. Subsequent blunt dissection of the periosteum along the myofascial space facilitated exposure of the metaphyseal end of the upper tibia. To optimize accessibility for the electric drill, several incisions were cautiously made with a sharp knife at the designated drilling site. The drilling trajectory, executed perpendicular to the proximal tibia, traversed through the bilateral cortical bone, yielding a transverse bone channel with a diameter of 2 mm. After drilling, meticulous removal of bone fragments ensued, followed by bilateral implantation of 2 mm-diameter, 8 mm-length nHA/PLLA absorbable screws, concomitant with the application of pressure to achieve hemostasis. Subsequent incision closure was accomplished through layered suturing techniques. It is noteworthy that all surgical procedures were performed by the same skilled individual. Post-operative care involved unrestricted activity post-anesthesia recovery, supplemented by daily intramuscular administration of 500,000 units of cefazolin sodium over a 3 days duration to mitigate the risk of postoperative infection. The nHA/PLLA absorbable screws employed in the study were sourced from Changchun Shengboma Biomaterials Co., LTD., constituting composite materials comprising nano-hydroxyapatite (nHA) and poly-L-lactic acid (PLLA).

DETECTION OF GENERAL INDICATORS

Routine weekly evaluations comprised monitoring changes in blood glucose levels, weight, food, water intake, and instances of morbidity or mortality. Blood specimens were acquired through tail pruning, facilitating subsequent analysis of random glucose levels utilizing a Sinocare glucose meter and test paper (Sinocare, China). Following surgical procedures, meticulous attention was devoted to disinfection, compression, and hemostasis of the tail wound.

HISTOLOGICAL AND HISTOMORPHOMETRIC ANALYSIS

Upon euthanasia at 4 weeks, 8 weeks and 12 weeks post-implantation, tissue samples were meticulously processed to obtain soft tissue sections 4 μ m thick and hard tissue sections 50 μ m thick. Hematoxylin-Eosin (HE) and Masson's trichrome staining were applied to the soft tissue sections, facilitating subsequent microscopic examination. Simultaneously, uncalcified hard tissue sections were meticulously prepared and subjected to quantitative analysis utilizing computer aided software (Leica Qwin

Image Processing and Analysis Software, Version 2.4, Amsterdam, the Netherlands) to assess the degree of interfacial osseointegration between absorbable screws and bone.

MICRO-CT SCANNING

The specimen is carefully positioned within a micro-computed tomography (Micro-CT) examination tank and securely immobilized to minimize any potential movement. Scanning was meticulously conducted along the longitudinal axis of the specimen. Specific scanning parameters were meticulously chosen: a 360° rotating scanning method, with a scanning duration of 17 min, an exposure time of 300 milliseconds, and a resolution of 9 μm . Following the completion of the scan, the 3D reconstruction of the bone trabecula surrounding the screw was meticulously carried out, delineating it as the region of interest. Quantitative analysis was meticulously conducted utilizing MicView V2.1.2 3D reconstruction processing software and ABA special bone analysis software. The specific measurement parameters are: (1) Bone volume fraction (BV/TV) is expressed by %, that is, bone volume (BV) divided by total volume (TV). (2) Trabeculae number (Tb.N) is expressed by 1/mm, which refers to the intersection point of bone and non-bone tissue of a given length, and can be understood as the number of bone trabeculae per mm distance. (3) Trabeculae thickness (Tb.Th) is expressed in μm to measure the average thickness of trabeculae cylinders. (4) Bone mineral density (BMD), expressed in mg/mm^3 , is the apparent density of the trabeculae structure of porous bone, reflecting the overall bone density of the region. (5) Connection density (CD) is expressed by $1/\text{mm}^3$, indicating the number of connections between trabeculae networks. (6) Trabeculae space (Tb.Sp) is represented by μm , that is, the average width of cavity between trabeculae bones. (7) Structural Model index (SMI), reflecting the degree of plate trabecula and columnar trabecula, indicating the structure of bone trabecula; The SMI of plate trabecula and rod trabecula were 0 and 3, respectively. When osteoporosis occurs, trabeculae bone changes from plate to rod shape and SMI value increases.

MICROINDENTATION MECHANICAL TESTING OF TRABECULAE BONE

Microindentation mechanical testing represents a reliable technique for evaluating the mechanical characteristics of bone tissue. This method entails quantifying the resistance encountered by a drill bit as it penetrates the bone tissue. In the current investigation, a microindentation test system (manufactured by FUTURE-TECH Company, Kanagawa Prefecture, Japan) was employed. The non-decalcified hard tissue sections obtained from rat specimens were meticulously positioned beneath a light microscope, with specific focus on the bone trabeculae region adjacent to

the absorbable screw for assessment. The instrument used a quadrangular Berkovich tip, the Angle between edge and center line was 77.05°, and the Angle between edge and center line was 65.3°. The maximum load was set to 100 mN, the retention time was 10 s, and the two diagonal lengths of the indentation were measured by microscope within 45 s of load removal. The trabeculae bonehardness (MPa) and elastic modulus (GPa) of bone trabeculae were calculated by the built-in software and the average value was calculated.

BIOMECHANICAL TEST

Upon euthanasia at 4 weeks, 8 weeks, and 12 weeks post-implantation, the tibia was meticulously dissected from both the upper and lower ends to ensure the removal of excess tissue. Following this, biomechanical evaluations were conducted by affixing the specimens onto a resin scaffold (pull-out experiment). The resin scaffold was securely fastened to the base of a biomechanical testing apparatus (BOSE 3220, Bose Corporation, USA), with the flat end of a 2 mm diameter cylindrical indenter connected to a 225 N sensor. Throughout the testing procedure, the cylindrical indenter and the absorbable screw were maintained perpendicular to the horizontal ground line, while the absorbable screw was displaced at a controlled speed of 0.1 mm/s. Subsequently, software (Version 1.2, Stuttgart, Germany) was employed to calculate the maximum pull-out force (N).

CONFOCAL RAMAN MICROSPECTROSCOPY

Confocal Raman Microspectroscopy (CRM) primarily captures the principal vibration frequencies of both organic and inorganic constituents within bone tissue. For this investigation, the bone trabeculae surrounding absorbable screws (non-decalcified hard tissue sections) were probed using the LabRAM Aramis Raman spectrometer (Horiba Jobin Yvon, France). The laser excitation wavelength is set at 785 nm, with an irradiation power of 100 mW on the sample surface, and an objective magnification of 50x is employed. Within bone tissue CRM analysis, the peak at 960 cm^{-1} signifies mineral content, while the peak at 856 cm^{-1} denotes collagen content. Consequently, the mineral-to-collagen ratio is determined by dividing the intensity of the 960 cm^{-1} peak by that of the 856 cm^{-1} peak.

WESTERN BLOT

The animals were euthanized 12 weeks post-implantation, and the absorbable screws were subsequently extracted for semiquantitative analysis. An adequate quantity of bone tissue surrounding the absorbable screw was homogenized with cell lysate and chilled on ice for 15 min. The specimens were centrifuged at 4 °C and 12,000 g for 10 min. The supernatant was aspirated, and the optical density was measured at 595 nm, followed

by protein concentration quantification using the BCA kit (Beyotime, Shanghai, China) colorimetric assay. The aliquots were then evenly distributed and stored at -20 °C. Protein isolation was conducted via SDS-PAGE, followed by electrophoretic transfer onto polyvinylidene fluoride membranes. Following sealing with 5% BSA/TBST for 1 h, the membrane was incubated with primary antibodies overnight at 4 °C. The following day, the membrane was washed with TBST before incubation with secondary antibodies (1:500 dilution, SAB, Baltimore, Maryland, USA) for 1 h. Subsequently, the membrane was rinsed with TBST. The membranes were then visualized, and imaging was conducted utilizing Quantity One software (Bio-Rad, Richmond, California, USA). Bone metabolic protein detection encompassed BMP-2, RUNX2, OPG, OCN, β -catenin, and ATF3.

STATISTICAL ANALYSIS

Data analysis was performed using SPSS22.0 (SPSS, Chicago, IL; Version 22.0). Descriptive statistics were employed to summarize all measured variables. Count data were presented as frequencies and percentages, while

measurement data were reported as mean \pm standard deviation ($\bar{x} \pm s$). Statistical differences between groups were calculated using t-tests or Mann-Whitney U test, with $P < 0.05$ considered statistically significant. Graphical representation of the statistical findings was generated using GraphPad Prism 9 (GraphPad Software, USA).

RESULTS

GENERAL CONDITIONS OF RATS AFTER MODELING

The blood glucose level, body weight, food intake and water intake of DM group and control group were significantly changed after injection (Table 1). No incidents of anesthesia mishaps were recorded during the surgical process, and the rats were able to resume lower extremity weight-bearing activities freely post-implantation. Upon observation, no discernible gait abnormalities were evident in either experimental group. Additionally, no significant incidences of incision infection were noted in the post-implantation rats. Following intraperitoneal injection of STZ in the DM group, gradual onset of DM symptoms was observed. Table 2 presents the blood glucose levels

TABLE 1. Blood glucose levels, body weight, 24 h food intake, and 24 h water intake for rats in the DM and control groups after injection ($\bar{x} \pm s$)

Monitoring indicators	Groups	Time points				
		Pre-injection	2 days	3 days	7 days	14 days
Blood glucose (mmol/L)	DM group	6.4 \pm 1.9	24.4 \pm 5.8*	24.1 \pm 3.2*	23.9 \pm 3.9*	21.7 \pm 4.2*
	Control group	6.5 \pm 2.3	6.4 \pm 1.5	6.8 \pm 2.5	6.5 \pm 1.4	6.6 \pm 2.3
Weight (g)	DM group	394.1 \pm 7.7	372.4 \pm 6.3*	360.6 \pm 7.3*	308.9 \pm 7.1*	290.3 \pm 8.2*
	Control group	393.8 \pm 6.9	392.2 \pm 7.2	390.8 \pm 6.9	391.5 \pm 5.7	390.8 \pm 7.4
Food intake (g/24 h)	DM group	27.4 \pm 4.2	29.9 \pm 4.9*	36.7 \pm 5.7*	52.3 \pm 9.4*	52.9 \pm 7.2*
	Control group	26.6 \pm 2.5	25.1 \pm 4.4	24.6 \pm 4.2	25.0 \pm 2.8	25.6 \pm 3.7
Water intake (g/24 h)	DM group	36.3 \pm 5.8	110.5 \pm 25.6*	123.8 \pm 33.5*	148.1 \pm 43.7*	150.8 \pm 45.8*
	Control group	35.8 \pm 5.9	34.7 \pm 6.4	35.6 \pm 5.5	36.5 \pm 7.1	36.2 \pm 7.2

* indicates $P < 0.05$ compared with control group. DM: diabetes mellitus

TABLE 2. Blood glucose and body weight of rats in DM group and control group before and after the implantation of absorbable screws ($\bar{x} \pm s$)

		Before implantation	1 week after implantation	4 weeks after implantation	8 weeks after implantation	12 weeks after implantation
Blood glucose (mmol/L)	DM group	21.7 \pm 4.2*	24.0 \pm 3.5*	24.4 \pm 5.6*	24.8 \pm 4.5*	25.3 \pm 6.3*
	Control group	6.6 \pm 2.3	6.7 \pm 2.7	6.5 \pm 3.3	6.5 \pm 2.2	6.5 \pm 3.8
Weight (g)	DM group	290.3 \pm 8.2*	289.4 \pm 7.1*	286.6 \pm 7.3*	290.5 \pm 6.5*	288.3 \pm 7.7*
	Control group	390.8 \pm 7.4	395.7 \pm 6.4	404.6 \pm 5.8	408.3 \pm 7.6	402.4 \pm 6.4

*indicates $P < 0.05$ compared with control group. DM: diabetes mellitus

and body weights of the rats in both groups before and after implantation. Out of the 45 rats in the DM group, 40 were successfully modeled while 5 failed. This yielded a modeling success rate of 88.9%. Notably, there were 3 deaths (6.67%) in the DM group and 1 death (3.33%) in the control group.

HISTOLOGICAL AND HISTOMORPHOMETRIC ANALYSIS

HE staining showed a progressive increase in new bone formation over time in both groups following absorbable screw implantation at 4 weeks, 8 weeks and 12 weeks post-implantation. Compared with the control group, the DM group had less new bone and poor trabeculae continuity at all time points after implantation (Figure 1(a)).

Masson's trichrome staining showed a gradual maturation of new bone tissue with prolonged implantation time. Specifically, at 4 weeks after implantation, the bone trabeculae surrounding the two group of absorbable screws exhibited clarity, albeit with loose arrangement and limited new bone formation. By 8 weeks and 12 weeks post-implantation, the trabeculae in both groups underwent reconstruction, gradually assuming a closer arrangement accompanied by new bone formation. However, at these time points, the bone trabeculae in the DM group displayed uneven arrangement, poor continuity, and more extensive blue-stained areas compared to the control group, indicative of lower bone maturity (Figure 1(b)).

Analysis of hard tissue sections showed the formation of new bone, which adhered to the oblique and concave walls of the screw threads at 4 weeks, 8 weeks and 12 weeks post-implantation in both groups. However, compared to the control group, the DM group exhibited a notable reduction in new bone formation around the absorbable screws, accompanied by thinner and discontinuous bone trabeculae (Figure 1(c)). Furthermore, the osseointegration area ratio of absorbable screw thread in the DM group was significantly lower than that in the control group at 4 weeks, 8 weeks and 12 weeks post-implantation (4W: $P = 0.049$; 8W: $P = 0.014$, 12W: $P = 0.012$) (Figure 1(d)).

MICRO-CT SCANNING

Visual inspection of the Micro-CT 3D reconstruction images showed a gradual increase in the number of bone trabeculae around the absorbable screws in both groups over time (Figure 2(a)). Micro-CT results depicted alterations in bone trabeculae microstructure and density parameters around absorbable screws in the two rat groups. At 4 weeks after implantation, there was no significant difference in the parameters of trabeculae bone between the two groups. At 8 weeks after implantation, BT/TV, Tb.N, Tb.Th, and BMD in DM group were significantly lower than those in control group (BT/TV: $P = 0.017$; Tb.N: $P = 0.046$; Tb.Th: $P = 0.043$; BMD: $P = 0.047$), while Tb.Sp

and SMI in DM group were significantly higher than those in control group (Tb.Sp: $P = 0.048$; SMI: $P = 0.025$). At 12 weeks after implantation, BT/TV, Tb.N, Tb.Th, BMD and CD in DM group were significantly lower than those in control group (BT/TV: $P = 0.003$; Tb.N: $P = 0.040$; Tb.Th: $P = 0.006$; BMD: $P = 0.012$; CD: $P = 0.044$), while Tb.Sp and SMI in DM group were significantly higher than those in control group (Tb.Sp: $P = 0.047$; SMI: $P = 0.032$) (Figure 2(b)-2(h)).

MICROINDENTATION MECHANICAL TESTING OF TRABECULAE BONE

At 4 weeks post-implantation, no significant differences were observed in the elastic modulus and trabeculae bonehardness between the two groups. However, at 8 weeks after implantation, the elastic modulus of bone trabeculae in the DM group was significantly lower than that in the control group ($P = 0.019$), while no significant difference was noted in trabeculae bonehardness between the two groups. By 12 weeks after implantation, both the elastic modulus and trabeculae bonehardness in the DM group were significantly lower than those in the control group (Elastic modulus: $P = 0.001$; Trabeculae bonehardness: $P = 0.014$) (Figure 3(a), 3(b)).

BIOMECHANICAL TEST

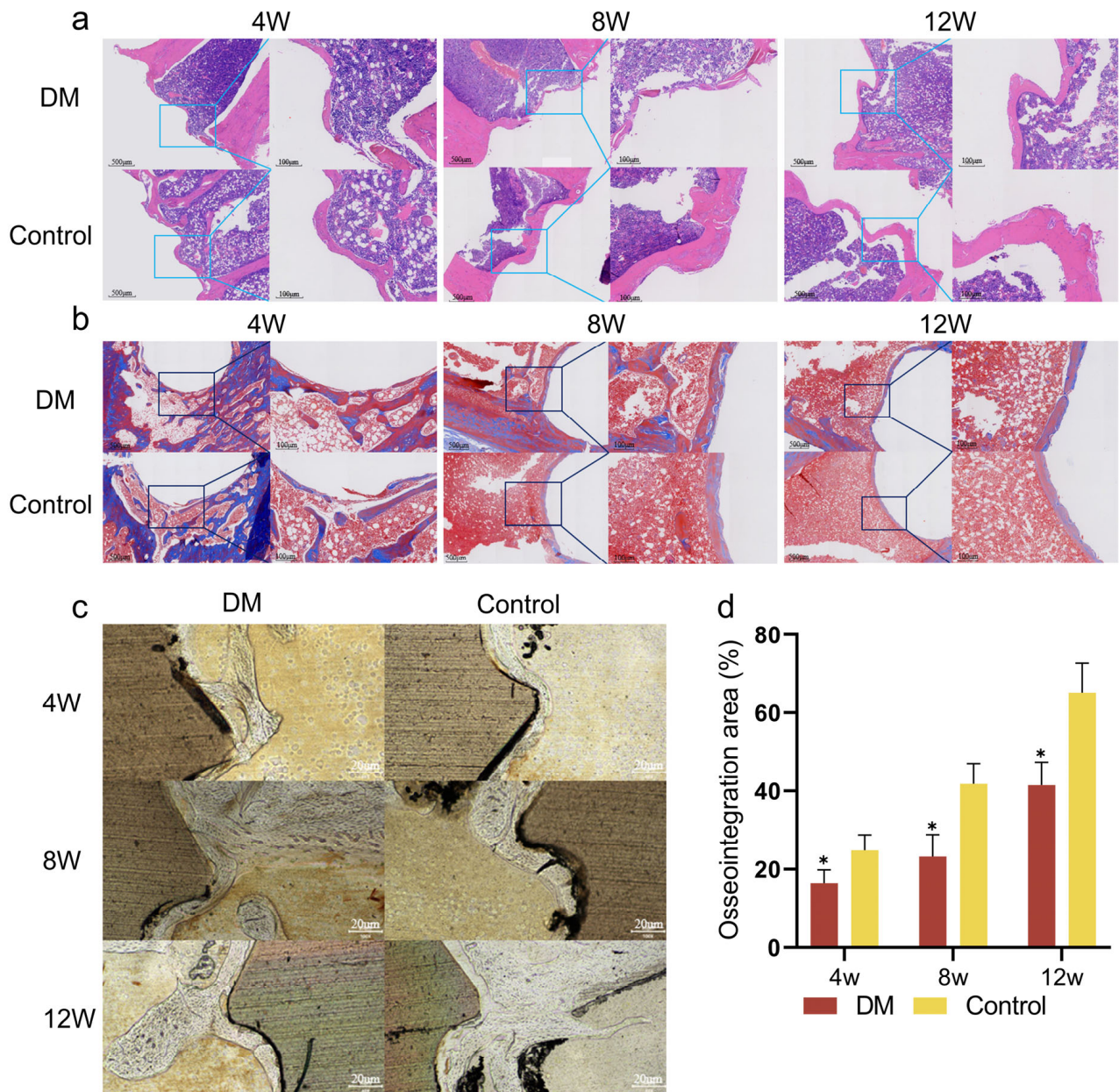
Biomechanical test showed that compared with the control group, the maximum load required for the pull-out of absorbable screws at 4 weeks, 8 weeks and 12 weeks after implantation was significantly reduced in the DM group (4W: $P = 0.014$; 8W: $P = 0.031$; 12W: $P = 0.017$) (Figure 3(c)).

CONFOCAL RAMAN MICROSPECTROSCOPY

CRM analysis showed that 4 weeks after implantation, there was no significant difference in bone trabeculae mineral/collagen ratio between the two groups. At 8 weeks and 12 weeks after implantation, the trabeculae mineral/collagen ratio in DM group was significantly lower than that in control group (8W: $P = 0.047$; 12W: $P = 0.006$) (Figure 3(d)).

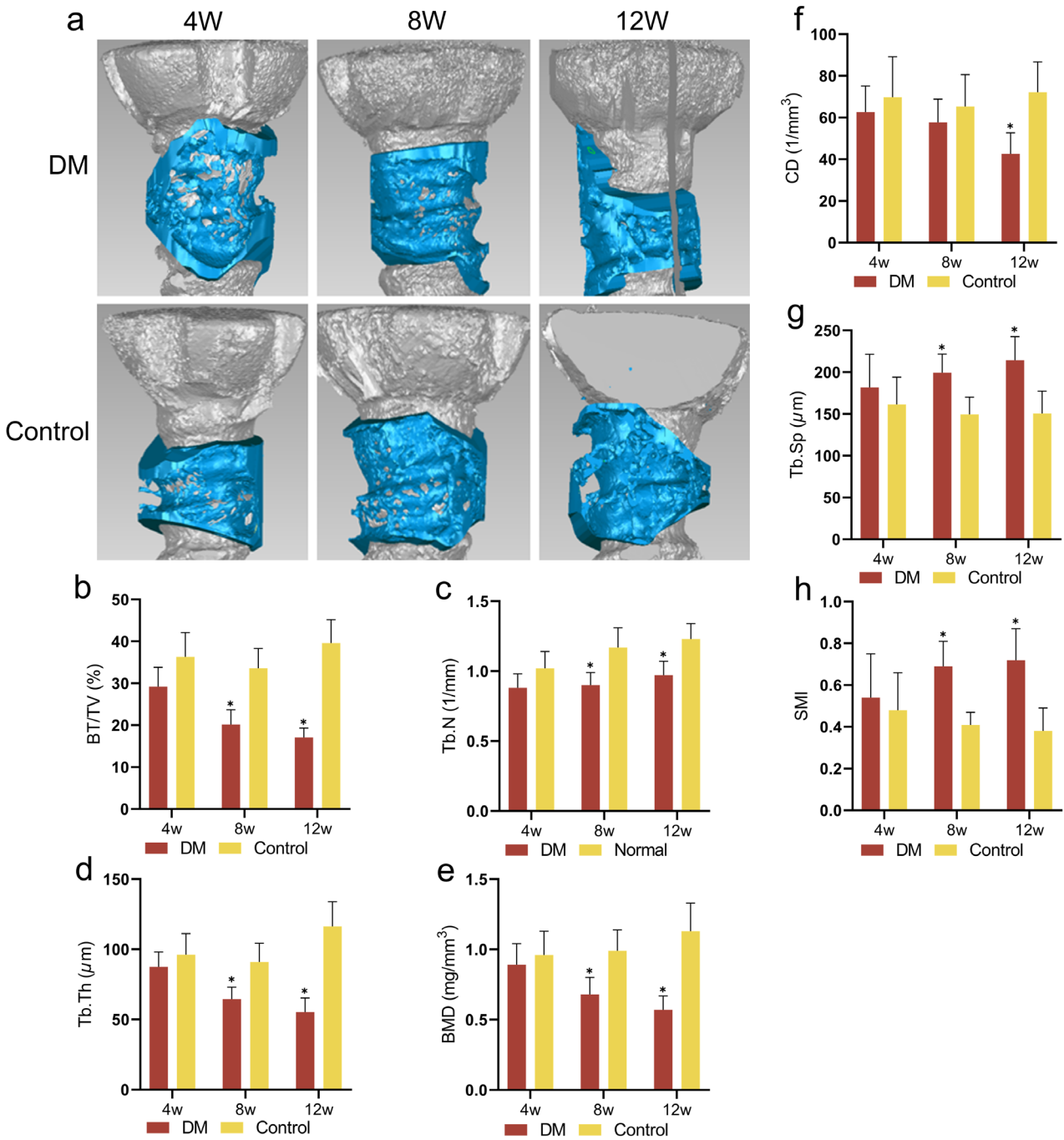
EXPRESSION LEVELS OF BONE METABOLISM-RELATED PROTEINS

At 12 weeks after implantation, the protein expression levels of BMP-2, RUNX2, OPG, OCN and β -catenin in the bone tissue around absorbable screws in DM group were significantly decreased compared with the control group, while the protein expression level of ATF3 was significantly increased, with statistical significance (BMP-2: $P = 0.047$; RUNX2: $P < 0.001$; OPG: $P < 0.001$; OCN: $P < 0.001$; β -catenin: $P < 0.001$; ATF3: $P < 0.001$) (Figure 3(e)-3(k)).



*indicates $P < 0.05$

FIGURE 1. Histological and histomorphometric analysis. (a) HE staining of the area around the absorbable screws in the DM and control groups at 4 weeks, 8 weeks, 12 weeks after implantation, (b) Masson's trichrome staining of the area around the absorbable screws in the DM and control groups at 4 weeks, 8 weeks, 12 weeks after implantation, (c) Hard tissue sections around the absorbable screws in DM and control rats at 4 weeks, 8 weeks, 12 weeks after implantation, and (d) The ratio of absorbable screw osseointegration area between DM and control rats



The data are shown as the mean ± SEM, *indicates P < 0.05. BT/TV: Bone volume fraction; Tb.N: Trabeculae Number; Tb.Th: Trabeculae thickness; BMD: Bone mineral density; CD: Connection density; Tb.Sp: Trabeculae space; SMI: Structural Model Index

FIGURE 2. Micro-CT 3D reconstruction results of trabeculae bone surrounding the absorbable screws in the two groups of rats. (a) Representative Micro-CT 3D reconstruction of peri-implant bone, the blue areas on the implant surface refers to the bone areas that contact the implant surfaces. (b-h) Quantitative analysis of trabeculae bone parameters regarding BT/TV, Tb.N, Tb.Th, BMD, CD, Tb.Sp and SMI

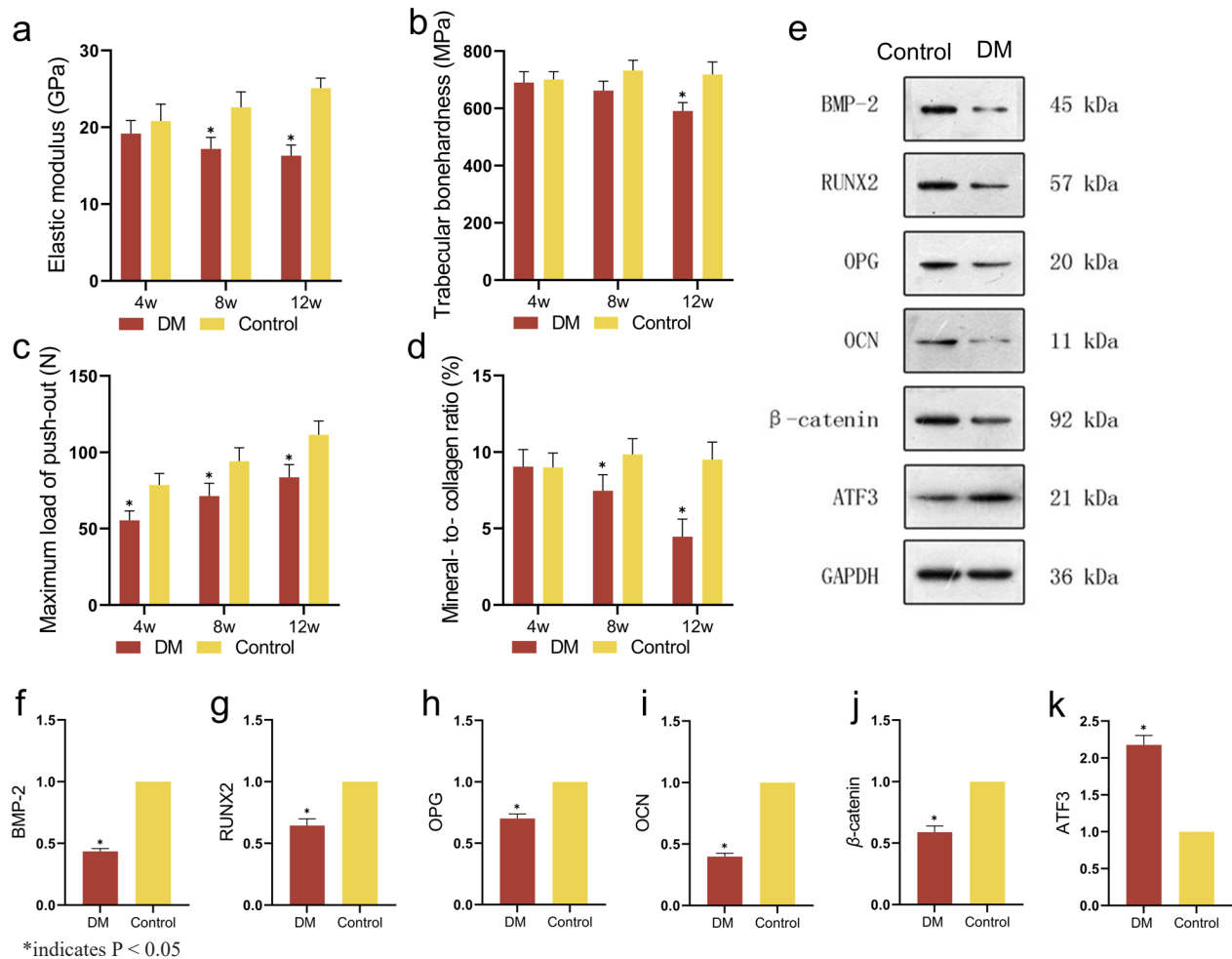


FIGURE 3. Biomechanical properties and molecular level studies. (a) Trabeculae elastic modulus of bone tissue around absorbable screws in rats, (b) Trabeculae bonehardness around absorbable screw in rats, (c) Maximum load of screw pull-out test in DM group and control group rats, (d) Comparative Raman spectroscopic analysis of trabeculae composition of bone tissue around absorbable screws in rats, and (e-k) Expression levels of bone metabolism-related proteins in bone tissue around absorbable screws in rats

DISCUSSION

In this longitudinal study, we used a variety of measurements at the microstructure (Histological, Histomorphometric analysis and Micro-CT scanning), micro and macro biomechanics (Microindentation mechanical testing of trabeculae bone and Biomechanical test) and molecular levels (Expression levels of bone metabolism-related proteins and the CRM test).

MICROSTRUCTURE

The evaluation of new bone formation and osseointegration around the implant serves as crucial indicators for assessing implant success. Prior research has highlighted that alterations in the bone environment induced by DM can impede osseointegration in regions of cortical bone

and bone marrow where titanium screws are implanted (Hasegawa et al. 2008). In our study, we initially employed HE staining, Masson's trichrome staining, and hard tissue sections to assess the capacity for new bone formation and osseointegration in the vicinity of absorbable screws. Results showed a gradual increase in new bone formation surrounding absorbable screws over time in both the DM and control groups. Notably, substantial differences were observed between 8 weeks and 12 weeks, with the DM group exhibiting lower numbers and maturity of new bone compared to the control group. Furthermore, analysis of hard tissue sections unveiled a significantly lower osseointegration area ratio of absorbable screws in the DM group compared to the control group at 4 weeks, 8 weeks, and 12 weeks post-implantation. Our findings suggest that nHA/PLLA absorbable screws are adversely affected by the DM skeletal environment.

Trabeculae bones typically exhibit a three-dimensional network structure. Under equivalent bone density conditions, a more optimal trabeculae bone structure confers superior biomechanical properties and stress resistance. This is attributable to the fact that, beyond bone mass alone, the geometric configuration of trabeculae bone determines its structural characteristics, consequently influencing its mechanical properties. DM can profoundly disrupt the structure of trabeculae and cortical bones. Burghardt et al. (2010) conducted a comparative analysis of bone microstructure between 19 patients with DM and 19 normal subjects using high-resolution quantitative peripheral CT, showing that radial cortical porosity was twice as high in DM compared to the control group. A recent case-control study involving 140 patients demonstrated that BV/TV, Tb.N and Tb.Th were diminished in individuals with DM relative to controls, while BV/TV was elevated, indicating a detrimental effect of DM on trabeculae structure (Giner et al. 2021). Similar findings have been corroborated in animal studies. DM rats exhibited significantly lower BV/TV, Tb.N and Tb.Th in the femoral head compared to the control group, and coupled with a notably increased Tb.Sp. With prolonged duration, the deleterious impact of DM on femoral head trabeculae structure became increasingly pronounced (Mohsin et al. 2019). In our research, morphological evaluation of bone trabeculae around absorbable screws via Micro-CT scanning showed significantly lower BV/TV, Tb.Th and BMD in the DM group compared to the control group, alongside significantly higher Tb.Sp and SMI values in the former. These findings suggest that DM disrupts the three-dimensional structure of bone trabeculae surrounding absorbable screws, leading to osteoporotic alterations, with the severity of osteoporotic changes exacerbated with prolonged DM duration.

BIOMECHANICS

Biomechanical properties serve as crucial indicators of implant osseointegration capacity. A case-control study showed that Young's modulus, toughness, ultimate stress, ultimate load, and external stiffness of trabeculae bone were markedly lower in DM patients compared to the control group (Giner et al. 2021). Additionally, another clinical investigation demonstrated that patients with DM exhibited reduced cortical volumetric bone density, thickness, and cross-sectional area, along with increased cortical porosity (Samelson et al. 2018). These findings collectively indicate the detrimental impact of DM on the mechanical properties of bone trabeculae, leading to compromised bone quality. DM may influence bone trabeculae mechanical properties through various mechanisms, including heightened non-enzymatic cross-linking of collagen fibers, accumulation of advanced glycation end products, and alterations in bone matrix properties (Brownlee 2005; Yamaguchi & Sugimoto 2011). In our study, we elucidated that DM significantly

diminished bone mass around absorbable screws through both global biomechanical and trabeculae bone microindentation mechanics tests, respectively. Moreover, the elastic modulus and trabeculae bonehardness in the DM group were significantly lower than those in the control group. Furthermore, the observed alterations in loose bone trabeculae on Micro-CT failure the mechanical properties of bone trabeculae. To the best of our knowledge, this study represents the first exploration of the impact of DM on osseointegration with bioabsorbable screws at the microscopic biomechanical level using microindentation.

MOLECULAR LEVEL STUDIES

Trabeculae composition plays a pivotal role in bone quality. In this investigation, CRM was employed to scrutinize the impact of DM on trabeculae composition. CRM operates on the principle of Raman scattering, enabling the extraction of molecular composition information of organic and inorganic substances by analyzing the scattering spectra of incident light across different frequencies. Renowned for its minimally invasive and non-invasive nature, CRM facilitates qualitative and quantitative analysis of samples. Previous literature underscores the utility of CRM in quantifying bone mineralization and matrix to evaluate bone quality, affirming its significance in bone tissue component studies. The bone matrix comprises inorganic minerals and organic collagen, where bone mineral content dictates bone strength and stiffness, while collagen influences bone malleability and toughness, crucial for withstanding deformation and energy absorption from external forces (Garnero et al. 2006). Typically, bone minerals constitute approximately 45% of bone volume, with collagen comprising about 40%, while the remaining 15% encompasses water bound to collagen or stored within the plumbing system. Interactions between minerals and collagen influence bone strength, with factors like degree of mineralization, collagen matrix proportion, crystal size, mineral and collagen formation rates, and their interrelationship collectively impacting bone strength. Animal experiments have demonstrated the influence of collagen content on bone mechanical properties, showing that stress deformation and energy absorption of bovine cortical bone correlate with collagen cross-linking level rather than bone mineral density (Garnero et al. 2006). Furthermore, clinical evidence underscores the close association between reduced bone mineral to collagen matrix ratio and hip fracture risk (Gerdhem et al. 2005). Our findings showed a significantly lower mineral/collagen ratio in bone trabeculae of the DM group compared to the control group, with this discrepancy amplifying over time. The diminished mineral/collagen ratio in bone trabeculae may underlie the observed decline in microindentation mechanics. Moreover, this study marks the first utilization of CRM tests to scrutinize the impact of DM on osseointegration with bioabsorbable screws at the molecular level.

Bone metabolism constitutes an ongoing cyclical process characterized by the dual activities of bone formation by osteoblasts and bone resorption by osteoclasts. Notably, bone metabolism in individuals with DM manifests as a low-turnover state characterized by diminished bone formation rather than heightened bone resorption. A 6-month study by Achemlal et al. (2005) on poorly controlled male patients with DM showed that serum osteocalcin levels were lower in DM patients compared to the control group, whereas no significant disparity was observed in serum C-terminal cross-linked terminal peptide levels between the two cohorts. This observation suggests a reduction in bone formation among DM patients while bone resorption remains unaltered. Moreover, blood glucose control levels also influence bone metabolic status, as evidenced by higher bone mineral density and lower bone metabolic rate in elderly women with DM compared to their non-diabetic counterparts, irrespective of insulin therapy administration (Gerdhem et al. 2005). The impact of DM on bone metabolism can be assessed through the examination of bone metabolic markers. In our study, the expression levels of bone metabolism-related proteins BMP-2, RUNX2, OPG, OCN, and β -catenin were markedly decreased in DM rats, whereas the expression levels of ATF3 protein, a negative regulator of osteoblast differentiation, were significantly elevated. These findings suggest impaired bone formation around absorbable screws in DM rats.

CONCLUSIONS

Collectively, our findings underscore the multi-faceted impact of DM on osseointegration with absorbable screws. DM not only disrupts trabeculae structure surrounding the absorbable screws and alters trabeculae bone composition, diminishing its mechanical properties, but also profoundly impacts bone quality surrounding the absorbable screws. Moreover, DM impedes new bone formation, compromises bone metabolism, and thereby impedes osseointegration at the absorbable screw-bone interface.

ACKNOWLEDGEMENTS

This research was funded by Hainan Province Clinical Medical Center ([2021] No. 276), Scientific research and cultivation fund of the Affiliated Shunde Hospital of Jinan University (No.202101002), Medical Scientific Research Foundation of Guangdong Province (A2023143), the Fundamental Research Funds for the Central Universities (21623319), the Funding of Science and Technology Projects in Guangzhou (SL2023A04J01317), Medical Joint Fund of Jinan University (YXJC2022005). The study was conducted in accordance with the Declaration of Helsinki, and approved by the Jinan University Animal Ethics Committee (20180531-07). The original contributions presented in the study are included in the article. Further inquiries can be directed to the corresponding authors.

Author contributions is as follows: ZW, LX, HH contributed equally. Conceptualization, ZW, LX, HH, LL, YG, JG, JC and LZ; methodology, ZW, LX, HH and ZC; software, ZW, LX and HH; validation, ZW, LX and HH; formal analysis, LL, YG, JG and JC.; investigation, LL, YG, JG and JC; resources, ZC; data curation, ZW and LX; writing - original draft preparation, ZW, LX and HH; writing - review and editing, XZ, SY and HW; visualization, ZW and ZC; supervision, GM and TM; project administration, XZ, SY and HW; funding acquisition, XZ, SY and HW. All authors have read and agreed to the published version of the manuscript.

REFERENCES

- Achemlal, L., Tellal, S., Rkiouak, F., Nouijai, A., Bezza, A., Derouiche E.M., Ghafir, D. & El Maghraoui, A. 2005. Bone metabolism in male patients with type 2 diabetes. *Clin. Rheumatol.* 24(5): 493-496. doi: 10.1007/s10067-004-1070-9
- Arama, Y., Salmon, L.J., Sri-Ram, K., Linklater, J., Roe, J.P. & Pinczewski, L.A. 2015. Bioabsorbable versus titanium screws in anterior cruciate ligament reconstruction using hamstring autograft: A prospective, blinded, randomized controlled trial with 5-year follow-up. *Am. J. Sports Med.* 43(8): 1893-1901. doi: 10.1177/0363546515588926
- Brownlee, M. 2005. The pathobiology of diabetic complications: A unifying mechanism. *Diabetes* 54(6): 1615-1625. doi: 10.2337/diabetes.54.6.1615
- Burghardt, A.J., Issever, A.S., Schwartz, A.V., Davis, K.A., Masharani, U., Majumdar, S. & Link, T.M. 2010. High-resolution peripheral quantitative computed tomographic imaging of cortical and trabecular bone microarchitecture in patients with type 2 diabetes mellitus. *J. Clin. Endocrinol. Metab.* 95(11): 5045-5055. doi: 10.1210/jc.2010-0226
- Corrêa, M.G., Ribeiro, F.V., Pimentel, S.P., Benatti, B.B., Felix Silva, P.H., Casati, M.Z. & Cirano, F.R. 2021. Impact of resveratrol in the reduction of the harmful effect of diabetes on peri-implant bone repair: Bone-related gene expression, counter-torque and micro-CT analysis in rats. *Acta Odontol. Scand.* 79(3): 174-181. doi: 10.1080/00016357.2020.1797159
- Galiveeti, M.R.V., El-Abed, K. & Ahmad, R. 2023. Early failure of primary total knee arthroplasty due to massive osteolysis caused by bio-absorbable interference screws. *Cureus* 15(4): e38143. doi: 10.7759/cureus.38143
- Garnero, P., Borel, O., Gineyts, E., Duboeuf, F., Solberg, H., Bouxsein, M.L., Christiansen, C. & Delmas, P.D. 2006. Extracellular post-translational modifications of collagen are major determinants of biomechanical properties of fetal bovine cortical bone. *Bone* 38(3): 300-309. doi: 10.1016/j.bone.2005.09.014

- Gerdhem, P., Isaksson, A., Akesson, K. & Obrant, K.J. 2005. Increased bone density and decreased bone turnover, but no evident alteration of fracture susceptibility in elderly women with diabetes mellitus. *Osteoporos. Int.* 16(12): 1506-1512. doi: 10.1007/s00198-005-1877-5
- Giner, M., Miranda, C., Vázquez-Gámez, M.A., Altea-Manzano, P., Miranda, M.J., Casado-Díaz, A., Pérez-Cano, R. & Montoya-García, M.J. 2021. Microstructural and strength changes in trabecular bone in elderly patients with type 2 diabetes mellitus. *Diagnostics (Basel)* 11(3): 577. doi: 10.3390/diagnostics11030577
- Hasegawa, H., Ozawa, S., Hashimoto, K., Takeichi, T. & Ogawa, T. 2008. Type 2 diabetes impairs implant osseointegration capacity in rats. *Int. J. Oral Maxillofac. Implants* 23(2): 237-246.
- International Diabetes Federation 2024. "Facts & figures." International Diabetes Federation Web, Last Modified 2024/5/5 (Accessed 5 May 2024). <https://idf.org/about-diabetes/diabetes-facts-figures/>
- Kim, S.H., Kim, D.Y., Kwon, J.E., Park, J.S. & Oh, J.H. 2015. Perianchor cyst formation around biocomposite biodegradable suture anchors after rotator cuff repair. *Am. J. Sports Med.* 43(12): 2907-2912. doi: 10.1177/0363546515608484
- Kwon, P.T., Rahman, S.S., Kim, D.M., Kopman, J.A., Karimbux, N.Y. & Fiorellini, J.P. 2005. Maintenance of osseointegration utilizing insulin therapy in a diabetic rat model. *J. Periodontol.* 76(4): 621-626. doi: 10.1902/jop.2005.76.4.621
- Macarini, L., Milillo, P., Mocchi, A., Vinci, R. & Ettore, G.C. 2008. Poly-L-lactic acid - hydroxyapatite (PLLA-HA) bioabsorbable interference screws for tibial graft fixation in anterior cruciate ligament (ACL) reconstruction surgery: MR evaluation of osseointegration and degradation features. *Radiol. Med.* 113(8): 1185-1197. doi: 10.1007/s11547-008-0334-x
- Mellado-Valero, A., Ferrer García, J.C., Herrera Ballester, A. & Labaig Rueda, C. 2007. Effects of diabetes on the osseointegration of dental implants. *Med. Oral Patol. Oral Cir. Bucal.* 12(1): E38-43.
- Mohsin, S., Kaimala, S., Sunny, J.J., Adeghate, E. & Brown, E.M. 2019. Type 2 diabetes mellitus increases the risk to hip fracture in postmenopausal osteoporosis by deteriorating the trabecular bone microarchitecture and bone mass. *J. Diabetes. Res.* 2019: 3876957. doi: 10.1155/2019/3876957
- Palumbo, R., Kuzma, S.A. & Flanigan, D.C. 2023. Failure of osteochondral lesions using bioabsorbable fixation in the adolescent patient: A case report. *J. isakos* 8(4): 267-272. doi: 10.1016/j.jisako.2023.05.005
- Samelson, E.J., Demissie, S., Cupples, L.A., Zhang, X., Xu, H., Liu, C.T., Boyd, S.K., McLean, R.R., Broe, K.E., Kiel, D.P. & Bouxsein, M.L. 2018. Diabetes and deficits in cortical bone density, microarchitecture, and bone size: Framingham HR-pQCT study. *J. Bone Miner. Res.* 33(1): 54-62. doi: 10.1002/jbmr.3240
- Shyng, Y.C., Devlin, H. & Ou, K.L. 2006. Bone formation around immediately placed oral implants in diabetic rats. *Int. J. Prosthodont.* 19(5): 513-514.
- Xiang, G., Huang, X., Wang, T., Wang, J., Zhao, G., Wang, H., Feng, Y., Lei, W. & Hu, X. 2020. The impact of sitagliptin on macrophage polarity and angiogenesis in the osteointegration of titanium implants in type 2 diabetes. *Biomed. Pharmacother.* 126: 110078. doi: 10.1016/j.biopha.2020.110078
- Xiao, L. 2019. Effect of diabetes mellitus on osseointegration of titanium screw. PhD Thesis, Jinan University (Unpublished).
- Yamaguchi, T. & Sugimoto, T. 2011. Bone metabolism and fracture risk in type 2 diabetes mellitus [Review]. *Endocr. J.* 58(8): 613-624. doi: 10.1507/endocrj.ej11-0063

*Corresponding author; email: zhengxiaofei12@163.com